THE ROYAL SOCIETY

Received 4 March 2003
Accepted 30 July 2003
Published online 5 April 2004

Recent developments in solid-state magic-angle spinning, nuclear magnetic resonance of fully and significantly isotopically labelled peptides and proteins

Suzana K. Straus

Department of Chemistry, University of British Columbia, 2036 Main Mall, Vancouver, British Columbia V6T 1Z1, Canada (*sstraus@chem.ubc.ca*)

In recent years, a large number of solid-state nuclear magnetic resonance (NMR) techniques have been developed and applied to the study of fully or significantly isotopically labelled (^{13}C, ^{15}N or ^{13}C/^{15}N) biomolecules. In the past few years, the first structures of ^{13}C/^{15}N-labelled peptides, Gly–Ile and Met–Leu–Phe, and a protein, Src-homology 3 domain, were solved using magic-angle spinning NMR, without recourse to any structural information obtained from other methods. This progress has been made possible by the development of NMR experiments to assign solid-state spectra and experiments to extract distance and orientational information. Another key aspect to the success of solid-state NMR is the advances made in sample preparation. These improvements will be reviewed in this contribution. Future prospects for the application of solid-state NMR to interesting biological questions will also briefly be discussed.

Keywords: solid-state NMR; peptide and protein labelling; magic-angle spinning; resolution; assignment strategies; structural parameters

1. INTRODUCTION

One of the main aims of structural genomics is to compile a database of representative protein structures. This information will serve as a catalyst for scientific discoveries in all areas of biological science, as recently reviewed by Burley (2000). Many methods are currently being developed in X-ray crystallography and nuclear magnetic resonance (NMR) spectroscopy to elucidate structures rapidly. Although solid-state NMR is not a high-throughput method, it may contribute significantly to the structural genomics effort by yielding information on proteins that do not easily form crystals or are not amenable to the application of solution-state NMR methods. Such systems include membrane proteins (Smith *et al*. 1996; Opella 1997; Griffin 1998; Davis & Auger 1999; de Groot 2000; Baldus 2002) and other fibrous proteins, such as amyloids (Tycko 2001), spider silk (Van Beek *et al.* 2002) and cellulose (Maunu 2002).

For solid-state NMR to be applicable to biomolecules, it is often essential that the protein or peptide be isotopically labelled, with either ^{13}C, ^{15}N or a combination thereof to enhance the sensitivity in the spectra. Unlike in solution-state NMR, the proton resonance alone is unsuited for resonance assignment of large biomolecules in the solid state, because even sophisticated resolution enhancement techniques such as combined rotation and multiple pulse spectroscopy (CRAMPS) do not reduce the linewidths sufficiently to achieve the resolution needed. However, with the use of higher magnetic fields and high magic-angle spinning (MAS) spinning speeds ($\nu_r \geqslant 30$ kHz), the use of the proton resonance will certainly increase, as recently reviewed in Schnell & Spiess (2001). Low-γ nuclei offer the advantage of smaller dipolar couplings and of larger chemical shift ranges than protons. As a result, good resolution can be achieved at moderate MAS spinning frequencies. This is the reason why ^{13}C and ^{15}N have, to date, been primarily used for studying peptides and proteins.

Many solid-state NMR studies have relied on the use of selective isotopic labelling of peptides and proteins, i.e. the introduction by chemical synthesis of a handful of isotopes, each at a specific position (e.g. C^{α} or CO) in a given amino acid residue. In certain systems, this level of labelling can also be achieved biosynthetically, by using selectively labelled amino acids as the source of nutrients during protein expression (K. M. Lee *et al*. 1995). This approach yields site-specific information, such as one or two distances or torsion angles between a small number of sites, while minimizing the number of interactions that contribute to line broadening. Examples on the use of selective labelling abound in the literature, demonstrating how this approach can be used to characterize cell wall synthesis (Cegelski *et al.* 2002) or binding sites in proteins (Watts *et al.* 2001) to name but two. This approach is not feasible, however, when a global and comprehensive structure of the peptide or protein is to be elucidated, because this would require the preparation of many samples, each labelled at a few sites. In this case, it is desirable to use full isotopic labelling, despite the ensuing reduction in resolution.

In recent years, a number of techniques have been developed to improve the resolution of spectra of fully or significantly isotopically labelled peptides and proteins.

This resolution must be as high as possible to extract the maximum amount of structural information from the spectra. Sample preparation has been found to significantly affect the resolution that can be achieved. In the following section, the approaches used to prepare optimal samples for MAS NMR, with the most advantageous labelling for the application, will be reviewed. Once samples are obtained, a number of correlation experiments can be used to assign the spectra. These different assignment strategies will be reviewed in § 3. Finally, methods used to obtain structural information, such as distances and torsion angles, will be discussed in § 4.

With these advancements, a number of structures have recently been solved from first principles. Examples include the fully $^{13}C/^{15}N$-labelled peptides Gly–Ile (Nomura *et al.* 2000) and Met–Leu–Phe (Rienstra *et al.* 2002*a*), and the fully $^{13}C/^{15}N$-labelled 62 residue protein, α-spectrin Src-homology 3 (SH3) domain (protein databank (PDB) entry: 1M8M (Castellani *et al.* 2002)). To compare, a number of structures have been solved using static NMR methods and macroscopically aligned samples: gramicidin (PDB entry: 1MAG (Ketchem *et al.* 1996)), M2 from the nicotinic acetylcholine receptor (1CEK (Opella *et al.* 1999)), fd bacteriophage Pvii coat protein (1MZT (Marassi & Opella 2003)), and the M2 H^+ channel from influenza virus (1MP6 (Wang *et al.* 2001), 1NYJ (Nishimura *et al.* 2002)). These structures were solved using either selectively or fully ^{15}N-labelled samples. To date, however, no structures of aligned samples that are fully $^{13}C/^{15}N$ labelled have been reported. With the recent methodological developments (e.g. Gu & Opella (1999) and references therein), there is no doubt that this should follow shortly. In this contribution, I will focus on the developments for fully or significantly $^{13}C/^{15}N$-labelled samples investigated by MAS NMR only.

2. SAMPLE PREPARATION

Prior to commencing a structural investigation of a peptide or protein by solid-state MAS NMR, samples need to be prepared. Two important considerations need to be taken into account: labelling and sample 'quality'. These aspects will be discussed in the following subsections.

(a) *Labelling strategies*

When working with labelled peptides or proteins, a choice must be made as to the level of labelling that best suits the application. As mentioned above, for investigations regarding local information on the biomolecule or even the substrate, labelling of a few sites is often more than sufficient. If, however, a comprehensive study is to be carried out, then a more significant portion of the peptide or protein must be labelled. Recently, an approach (Hong 1999*a*; Hong & Jakes 1999) was presented that relies on a combination of selective[1] and extensive ^{13}C labelling. Selective labelling is achieved by using glucose or glycerol labelled in the [1,3]- or [2]-position as the sole carbon source in protein expression (LeMaster 1994). The manner in which the isotopic labels are incorporated in the different amino acids depends on which enzymatic pathway is used to generate the precursors in the biosynthesis. The required pathways are glycolysis, the citric-acid cycle and the pentose phosphate pathway (Stryer 1988). Extensive ^{13}C labelling is achieved in the same manner, but with fully labelled glucose or glycerol as the only carbon source. By analogy, uniform ^{15}N labelling is achieved by using ^{15}N-labelled ammonia as the sole nitrogen source. This approach of using a set of two or three samples with different labelling patterns was used successfully by Castellani *et al.* (2002) for the assignment and structure determination of the SH3 domain.

In the future, other labelling strategies, such as those currently used in solution-state NMR (reviewed in Goto & Kay 2000), may also become increasingly important. For example, deuterium labels have been used extensively in solution-state NMR studies of protein structure and dynamics (Ottleben *et al.* 1997; Gardner & Kay 1998; Goto *et al.* 1999; Richter *et al.* 1999; Goto & Kay 2000; Morgan *et al.* 2000). By labelling a significant portion of the protein backbone and/or side-chains, it is possible to edit out specific ^1H signals from areas of interest in the protein, such as a binding site (Shan *et al.* 1998). By using this approach, the molecular mass limit of proteins that can be studied using solution-state NMR has effectively increased from 10–15 kDa protein systems to 40–65 kDa protein systems, thus broadening the range of interesting biological questions that can be tackled using liquid-state NMR. In solid-state NMR, deuteration has also been used extensively to obtain structural and dynamic information (for some recent examples see Lee *et al.* 1999; Moltke *et al.* 1999; Geahigan *et al.* 2000; Middleton *et al.* 2000). In contrast to the situation in solution-state NMR, however, the deuterium labels in solid-state NMR are typically directly observed. Deuterium labels could, however, also be used to simplify solid-state spectra of proteins labelled with deuterium, or in the case of membrane proteins to eliminate the signal arising from the lipids. An example of the former can be found in Reif *et al.* (2001) and also in Samoson *et al.* (2001) on malonic acid, whereas an example of the latter application is illustrated in figure 1, where the M13 coat protein, labelled at positions [2-^{13}C]Val29 and [1-^{13}C]Val30, was reconstituted in 1,2-dimyristoyl-sn-glycero-3-phosphocholine (DMPC) (figure 1*a*) and DMPC-d67 (figure 1*b*). It can clearly be seen how the spectra can be simplified. Although this spectral editing is not critical for this particular peptide sample, it is quite important if the peptide is fully ^{13}C labelled, as in this case spectral overlap would be a problem.

A further example of the potential extension of labelling strategies used in solution-state to those used in solid-state NMR is the use of intein-mediated ligation (Perler 1998). This technique involves the use of genes found in prokaryotes or lower eukaryotes, which contain an in-frame open reading frame, which in turn encodes an internal protein (intein). These inteins are cleaved off after translation and are then ligated to a target protein by a splicing reaction (Yamazaki *et al.* 1998). This allows segments of the protein to be isotopically labelled while others are left unlabelled (Otomo *et al.* 1999*a*,*b*; Blaschke *et al.* 2000; Cowburn & Muir 2001). This effectively reduces the size of the protein to one where NMR techniques can be directly applied. For solid-state applications, one can imagine a labelling strategy where a set of two or three samples is used: one uniformly $^{13}C/^{15}N$-labelled sample and one $^{13}C/^{15}N$-labelled sample for each 20–40-residue

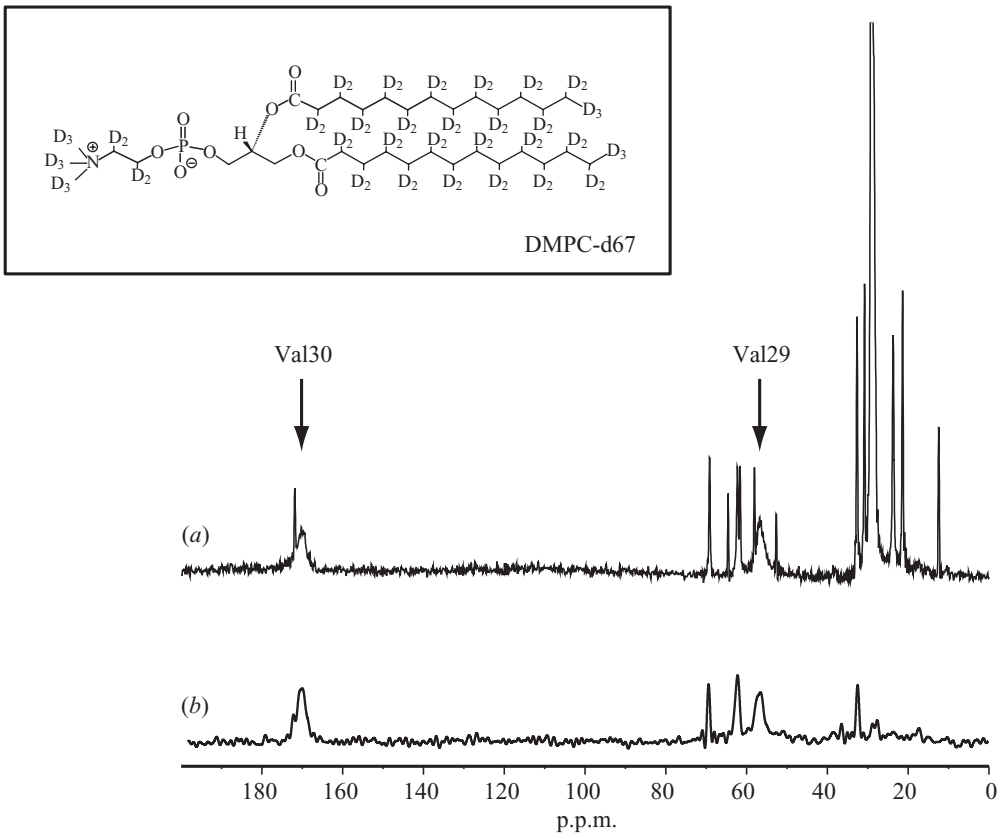

Figure 1. ^{13}C-CPMAS spectra of M13, labelled at [2-^{13}C]Val29 and [1-^{13}C]Val30, reconstituted in (*a*) protonated DMPC and (*b*) deuterated DMPC-d67 (shown in inset). Both spectra were recorded with spinning speeds of 10 kHz and a cross-polarization contact time of 2.5 ms. (C. Glaubitz, S. K. Straus and A. Watts, unpublished data.)

segment. This approach remains to be tested experimentally.

(**b**) *Resolution enhancement by recrystallization*

Once the peptide or protein has been isotopically labelled, either through chemical synthesis (for small peptides) or by protein expression, a lyophilized powder of (often) pure material is obtained. In such powdered samples, variations in the orientation and shape of the different crystallites present can give rise to local fields (Alla & Lippmaa 1982; Schwerk *et al.* 1996). These fields, in turn, give rise to line broadening, some of which can be removed by MAS. Others, however, such as those that arise through the effects of sample packing, cannot be averaged out by sample spinning. In this case, sample recrystallization and hydration can be used to improve molecular packing. An example of this is demonstrated in figure 2, which shows the effect of recrystallization in the ^{13}C linewidth in cross-polarization magic angle spinning (CPMAS) spectra of unlabelled antamanide. The top spectrum (figure 2*a*) shows the resolution that can be achieved from a lyophilized powder. The lower spectrum (figure 2*b*) was obtained from a sample of antamanide that was recrystallized from a 7 : 3 methanol : water mixture, under conditions of slow evaporation. The resulting needle-like crystals were ground prior to being inserted in the MAS rotor. A similar comparison was made by Detken *et al.* (2001) for antamanide. They also found optimal resolution for antamanide recrystallized under the same conditions of methanol : water to yield needle-like crystals. In their case, however, the resolution obtained is somewhat better because antamanide was trapped into a single isoform. As with other dynamic peptides, the conformation of antamanide can be quite variable (Wieland & Bodanszky 1991). Moreover, water content and hydrogen bonding networks are also quite variable from antamanide sample to antamanide sample (Karle 1986). This most probably partly[2] accounts for the differences observed in the spectra obtained by Straus *et al.* (1997) and Detken *et al.* (2001). Regardless, both studies demonstrate that antamanide can be assigned using solid-state NMR techniques. For larger proteins, recrystallization is also of importance as demonstrated by Belton *et al.* (1993) for hen egg white lysozyme. Careful recrystallization and monitoring of the water content of the protein sample resulted in a halving of the linewidth of the resonance at 17 p.p.m. in a ^{13}C-CPMAS spectrum of lysozyme.

As in crystallography, the addition of precipitants to promote crystallization, such as non-chaotropic salts, polymers (e.g. polyethylene glycol (PEG)), polyalcohols, organic solvents (Berry 1995) and saccharides, are also helpful for solid-state NMR applications. For instance, Studelska *et al.* (1996) found that the addition of PEG-8000 and sucrose gave rise to homogeneous lineshapes of the protein complex 5-enolpyruvylshikimate-3phosphate synthase/shikimate-3-phosphate/glyphosate being investigated. Pauli *et al.* (2000) found a similar improvement in the resolution of the solid-state NMR spectra of α-spectrin SH3 domain upon addition of PEG-8000 and sucrose. They also found, however, that precipitation of the protein from a solution of ammonium sulphate yielded even better resolved ^{13}C-CPMAS spectra. Similar findings have also

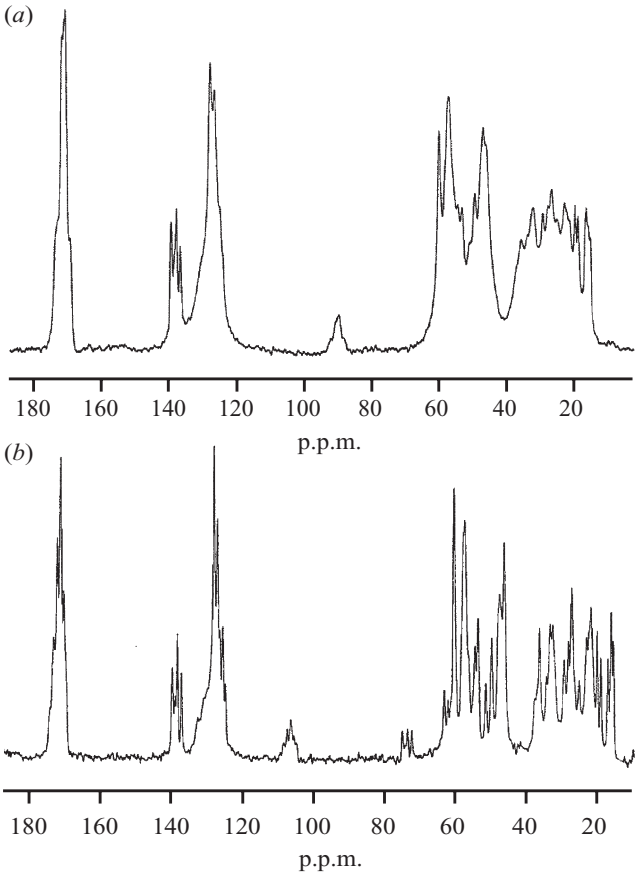

Figure 2. ^{13}C-CPMAS spectra of unlabelled antamanide: (*a*) before recrystallization; (*b*) after recrystallization from a mixture of methanol : water (7 : 3).

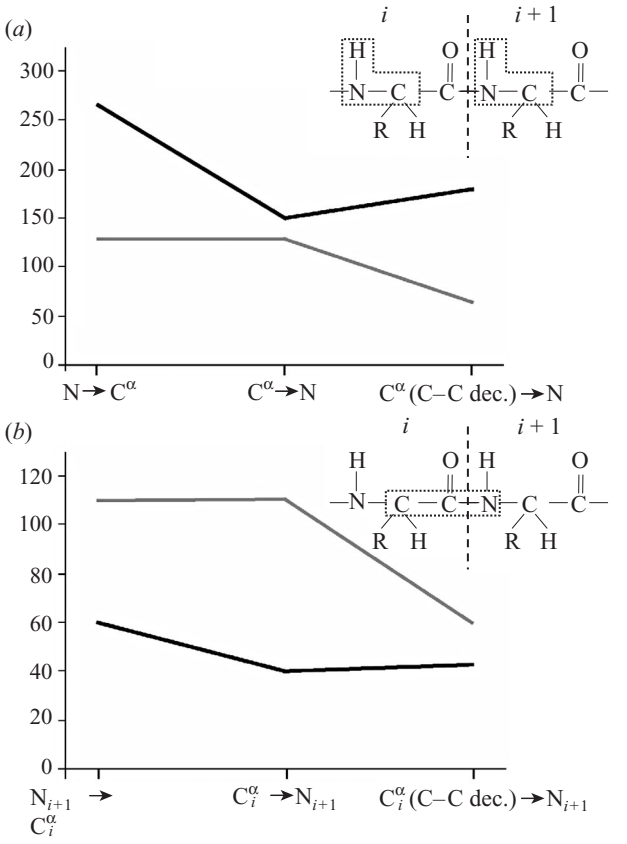

Figure 3. Comparison of the S/N ratios (black lines) and linewidths (grey lines), measured as the full width at half height (FWHH) in hertz on a 9.4 T spectrometer. (*a*) For the intra-residue experiments correlating N with C^{α}. X → Y refers to an experiment where Y is the detected nucleus. C–C decoupling (dec.) refers to the application of the homonuclear J-decoupling method described in Straus *et al.* (1996). (*b*) For the inter-residue experiments correlating N from residue $i + 1$ with C^{α} from residue i. The S/N ratios decrease in going from a ^{13}C- to a ^{15}N-detected experiment by a factor of 1.5. The use of homonuclear decoupling reduces the linewidths by a factor of approximately 2. (Adapted from table 1 in Straus *et al.* (1998).)

been reported in Jakeman *et al.* (1998) and Martin *et al.* (2003). Recently, 2-methyl-2,4-pentanediol (MPD), which has properties midway between those of low-molecular-mass PEG molecules and organic solvents (Berry 1995), has also been shown to be useful for solid-state NMR applications (McDermott 2002). This small polyalcohol displaces water in grooves and cavities on the surface of the protein and promotes stabilization by preferential hydration (Anand *et al.* 2002). It can be used as a cryoprotectant, as well as a precipitant, and in some cases is found to act as a denaturant (Arakawa *et al.* 1990). In future solid-state NMR applications, combinations of precipitants may also prove to be useful: e.g. ammonium sulphate or sodium citrate (major precipitant) plus additives (0.5–6%) such as PEG 400–2000, MPD, ethanol or methanol. Regardless of the specific recrystallization conditions used, the quality of the sample is key to any assignment strategy. Without high resolution, it is very difficult to obtain complete structural information from uniformly labelled samples.

3. ASSIGNMENT STRATEGIES

In recent years, a large number of solid-state NMR methods used for the full assignment of ^{13}C- or ^{13}C/^{15}N-labelled peptides and proteins have been developed. Many of the approaches are closely related to methods used in liquid state, where such experiments as HCACO, HNCO, HNCA and H(CACO)N are routinely used (Croasmun & Carlson 1994, pp. 916–926). In the solid state, three main types of correlation experiment are used: ^{13}C–^{13}C, ^{13}C–^{15}N and, more recently, ^{13}C–^{1}H or ^{15}N–^{1}H correlations. These techniques are all either two-dimensional (2D) or higher-dimensional experiments (table 1). A more complete theoretical description of each of these methods can be found in the many references in table 1 and also in a recent review (Baldus 2002).

The choice of experiments needed to fully assign a peptide or protein depends on a number of factors. The first of these is, as mentioned previously, the level of labelling of the peptide or protein. For instance, in Straus *et al.* (1997), the cyclic decapeptide antamanide was only ^{13}C labelled. The assignment strategy was thus based solely on ^{13}C–^{13}C correlations, applied to a single sample. More specifically, intra-residue correlations were obtained from a proton-driven spin diffusion (PDSD) (table 1) experiment with short mixing time and inter-residue correlations were obtained from a PDSD experiment with a long mixing time. Alternatively, an assignment strategy based on combined data from ^{13}C–^{13}C correlations and ^{13}C–^{1}H

Table 1. Summary of some of the ^{13}C–^{13}C, ^{13}C–^{15}N and ^{13}C–^{1}H (or ^{15}N–^{1}H) correlation experiments used to assign spectra of uniformly labelled peptides and proteins. For a more comprehensive list, the recent reviews by Griffin (1998) and Baldus (2002) should be consulted.

correlation	experiment[b]	reference
^{13}C–^{13}C	PDSD	Suter & Ernst (1985)
	RFDR	Bennett *et al.* (1992)
	J-HOHAHA	Ramamoorthy *et al.* (1993)
	DRAMA	Tycko & Smith (1993)
	HORROR	Nielsen *et al.* (1994)
	DRAWS	Gregory *et al.* (1995)
	MELODRAMA	Sun *et al.* (1995*a*)
	C7	Y. K. Lee *et al.* (1995)
	TOBSY	Baldus & Meier (1996)
	INADEQUATE	Lesage *et al.* (1997)
	DREAM	Verel *et al.* (1998)
^{13}C–^{15}N	RFDRCP	Sun *et al.* (1995*b*)
	APHH-CP	Baldus *et al.* (1996)
	CAN, $N_{i+1}(CO)CA_i$ & $CA_i(CO)N_{i+1}$	Straus *et al.* (1998)
	SPECIFIC-CP	Baldus *et al.* (1998)
	N(CO)CA & NCACB	Hong (1999*b*)
	N(CA)CB & N(CO)CA	Detken *et al.* (2001)
	soft-CACO NCA & *soft*-CA NCOCA[a]	Astrof & Griffin (2002)
^{13}C–^{1}H	FSLG HETCOR	van Rossum *et al.* (1997)
(or ^{15}N–^{1}H)	^{1}H detected HETCOR	Ishii *et al.* (2001)
	PMLG HETCOR	Vinogradov *et al.* (2002)

[a] These experiments can also be used to establish ^{13}C–^{13}C correlations.
[b] Definitions of these terms can be found in the referenced papers.

correlations can be applied to samples that are only ^{13}C labelled. This was recently demonstrated for chlorophyll *a* (Van Rossum *et al.* 2002). The advantage of using the ^{1}H resonance is the higher sensitivity of this nucleus compared with carbon ($\gamma_H/\gamma_C = 4$) and the long-range nature of the ^{13}C–^{1}H dipolar interaction. If the peptide or protein is both ^{13}C and ^{15}N labelled, then typically the assignment strategy relies on datasets from ^{13}C–^{13}C intra-residue correlations, ^{13}C–^{15}N intra-residue correlations (e.g. correlating N from residue i with C^{α} from the same residue) and ^{13}C–^{15}N inter-residue (e.g. correlating N from residue $i+1$ with C^{α} from residue i) correlations. This type of approach was applied to antamanide (Detken *et al.* 2001), ubiquitin (Straus *et al.* 1998; Hong 1999*b*), bovine pancreatic trypsin inhibitor (BPTI) (McDermott *et al.* 2000) and the SH3 domain (Pauli *et al.* 2001).

Another important consideration when choosing an assignment strategy is sensitivity. As already mentioned, one distinct advantage of using ^{13}C–^{1}H correlations is the higher sensitivity of ^{1}H. This was clearly demonstrated by Ishii *et al.* (2001), where a comparison was made between a ^{13}C-detected ^{13}C–^{1}H heteronuclear correlation (HETCOR) experiment and a ^{1}H-detected version of the same experiment. An enhancement of $\sqrt{5}$ in signal-to-noise (S/N) for a sample of amyloid fibrils was found. For ^{13}C–^{15}N correlation experiments, sensitivity must also be taken into account. A comparison of S/N ratios obtained for a fully $^{13}C/^{15}N$-labelled dipeptide (Val-Phe) is given in figure 3 (Straus *et al.* 1998). In figure 3*a*, a comparison is made between ^{13}C-detected ($N \rightarrow C^{\alpha}$) and ^{15}N-detected experiments correlating the intra-residue nitrogen and the alpha carbon. The loss in sensitivity in going to ^{15}N detection is a factor of 1.5, which is close to the theoretical value of

$$\frac{(S/N)_C}{(S/N)_N} = \frac{\gamma_C^{3/2} T_{2,C} f}{\gamma_N^{3/2} T_{2,N}} = 1.41,$$

where γ_N and γ_C are the gyromagnetic ratios of ^{15}N and ^{13}C, respectively, the T_2 values correspond to the measured linewidths of the ^{15}N and ^{13}C linewidth in a single pulse experiment and f is a factor that accounts for different channel sensitivities on a given spectrometer (Straus *et al.* 1998). In figure 3*b*, a similar factor of 1.5 is found between the ^{13}C- and ^{15}N-detected inter-residue correlation experiments. A comparison between the one-bond transfer (intra) (figure 3*a*) and the two-bond transfer (inter) (figure 3*b*) experiments clearly shows that there is a factor of 4 in loss in sensitivity. This factor of 4, which translates into an increase in experimental time for the two-bond transfer experiment by a factor of 16, is an important consideration when going from a 2D to a three-dimensional (3D) experiment. It could be improved by using more efficient pulse sequences to transfer magnetization between the ^{13}C nuclei (Baldus 2002).

Finally, resolution will also have an impact on the choice of assignment strategy. If the resolution is not sufficiently high to clearly resolve the resonances in a 2D experiment, then higher-dimensional experiments are needed. As mentioned above, this may come at the price of sensitivity, because multiple polarization transfers are required. In recent work (Astrof *et al.* 2001; Luca & Baldus 2002), however, the possibility of reducing higher-dimensional experiments to 2D experiments was presented. This is achieved by using reduced dimensionality experiments, first developed in liquid-state NMR (Szyperski *et al.* 1993; Brutscher *et al.* 1994). The method relies on the simultaneous incrementation of two or more indirect evolution periods (t_1, t_2,...) and results in spectra

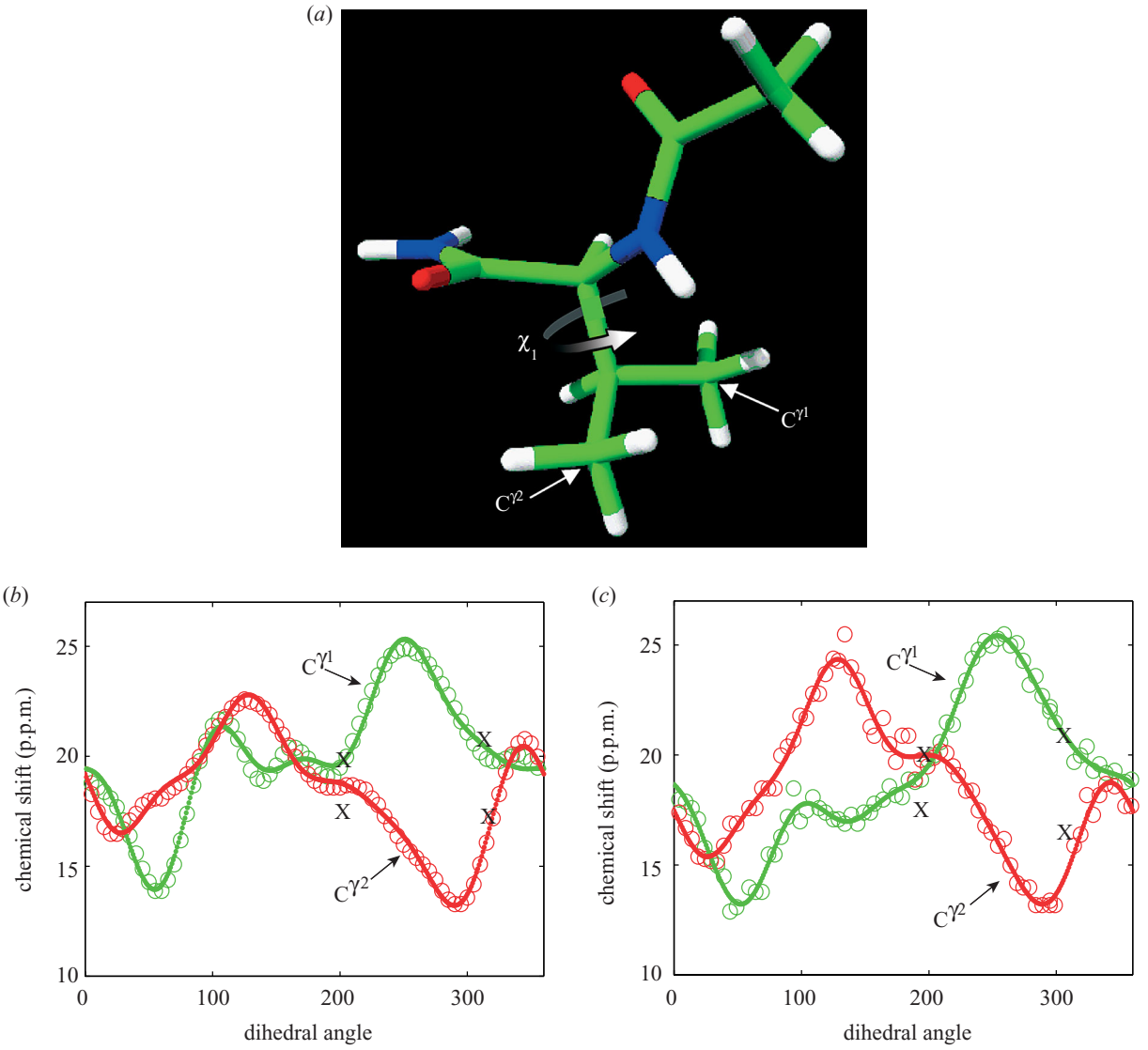

Figure 4. Comparison of SOS-DFPT-calculated valine $C^{\gamma 1}$ and $C^{\gamma 2}$ chemical shifts with the shifts determined from solid-state NMR experiments on antamanide, where two χ_1 rotamers were found to coexist in the sample (Straus *et al.* 1997). (*a*) Minimal fragment used in the density functional theory (DFT) calculations (see text). (*b*) Chemical shift values obtained using a rigid fragment. In green and red (open circles, calculated; line, best fit of calculated data) are the values for $C^{\gamma 1}$ and $C^{\gamma 2}$, respectively. The black crosses are the experimentally determined chemical shifts (two for $C^{\gamma 1}$ for rotamer I and II; two for $C^{\gamma 2}$ for rotamer I and II (Straus *et al.* 1997)). (*c*) Chemical shift values obtained using energy-minimized structures. The colour coding is the same as in (*b*).

where a given resonance centred at Ω_1 is split into a sum and difference shift of $\Omega_1+\kappa\Omega_2$ and $\Omega_1-\kappa\Omega_2$, where Ω_2 is the chemical shift of another resonance and $t_2=\kappa t_1$. For example, in Astrof *et al.* (2001), Ω_1 was chosen to be the CO resonance and Ω_2 was chosen to be the N resonance in a CO N CA experiment (Croasmun & Carlson 1994, pp. 916–926). Thus the resulting 2D correlation relates $\Omega_{CO}+\Omega_N$ and $\Omega_{CO}-\Omega_N$ to the alpha carbon chemical shift of the same residue. Knowledge of either the N or CO chemical shift, obtained in a separate experiment, then results in the determination of the shift of the other. When compared with 3D methods, the sensitivity of reduced dimensionality experiments is the same, namely a factor of $\sqrt{2}$ with respect to conventional 2D experiments. This is valid as long as the symmetry of the peak pairs is taken into account when peak picking (Brutscher *et al.* 1995). Thus, the advantage in the reduced dimensionality experiments does not lie in improved sensitivity. Rather, the benefit of reducing the number of dimensions comes from the fact that the digital resolution and the spectral resolution can be similar in 2D experiments, whereas in 3D or higher-dimensional experiments the digital resolution is much smaller. This has an important consequence for the resolution in the spectra.

4. STRUCTURAL PARAMETERS

Once the resonances in the NMR spectra have been assigned, structural constraints can be extracted to gain insight into the secondary structure of the peptide or protein. To this end, three main classes of experiment can be used: experiments that measure conformation-dependent chemical shifts, experiments that yield torsion angles and, finally, experiments where interatomic distances can be determined. Each of these categories will be discussed briefly in the following subsections.

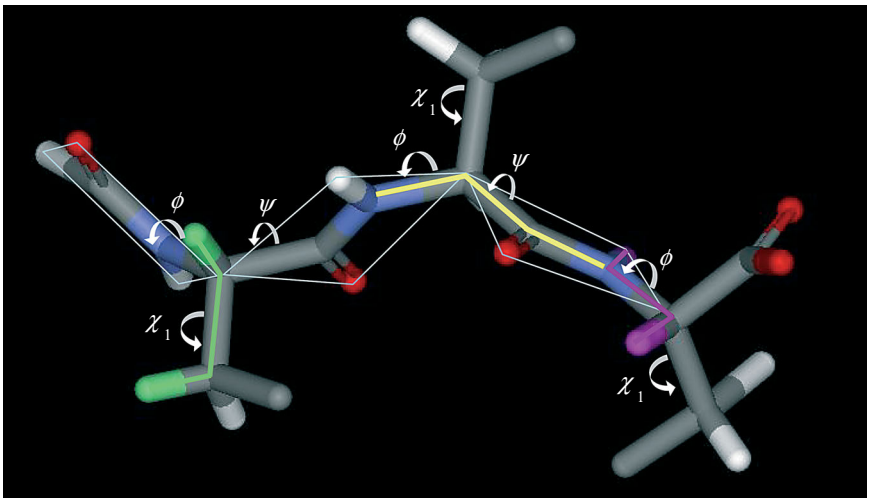

Figure 5. Tripeptide structure showing the backbone (ϕ, ψ) and side-chain (χ_1) dihedral angles. The 3D NMR correlation experiments needed to determine these angles are shown with thick lines: (yellow) N_i–CA_i–CO_i–N_{i+1} yields ψ; (purple) H_i–N_i–CA_i–HA_i yield ϕ; and (green) HA_i–CA_i–CB_i–HB_i yields χ_1.

(a) *Chemical shift*

The chemical shift is a sensitive measure of the electronic environment that surrounds a nucleus. Many studies, in both solution-state NMR (Wishart *et al.* 1991; Cornilescu *et al.* 1999; Ma *et al.* 2002; Labudde *et al.* 2003) and solid-state NMR (Shoji *et al.* 1993; Saito *et al.* 2000; Williamson *et al.* 2002), have clearly illustrated how the chemical shift can be used to qualitatively determine the conformation of peptides and proteins. In addition, several studies have demonstrated how such interactions as hydrogen bonding affect the chemical shift anisotropy (CSA) (Wei *et al.* 1999; Brender *et al.* 2001). Recently, Baldus (2002) compared the isotropic chemical shifts measured for SH3 in the solid state with random coil values, in a manner analogous to that used in solution-state NMR (Wishart *et al.* 1991). It was found that no strong correlation exists between the chemical shift differences for CO, N and CA (denoted Δ_{CO}, Δ_N and Δ_{CA} here) and the secondary structure elements in the SH3 domain. The best correlation was obtained only if both the values of CA and CB were considered together, i.e. $\Delta_{CA-CB} = \Delta_{CA} - \Delta_{CB} = [\delta_{CA} - \delta_{CB}]_{observed} - [\delta_{CA} - \delta_{CB}]_{random\_coil}$. By measuring these difference frequencies Δ_{CA-CB} experimentally, Luca & Baldus (2002) were able to tentatively assign the ^{13}C resonances of ubiquitin given the known secondary structural elements. The CSA can also be used to glean information on secondary structure, as recently demonstrated by Hong. The solid-state NMR experiments described in Hong (2000) can be used for determining the width of the CSA tensor for alpha carbons. This can then be related to secondary structural elements by comparing the decay of intensity of the C^α resonance over time with simulated values for known secondary structural elements.

With the recent developments in quantum mechanical calculations of NMR parameters (e.g. Malkin *et al.* 1996; Havlin *et al.* 1997; Case 2000), it may be foreseeable that in the future the conformation of a backbone or a side-chain may be determined by comparing experimental chemical shifts with calculated ones. An example of that is shown in figure 4 for the valine side-chain in antamanide (Straus 1998). Figure 4*a* shows the molecular fragment used for the sum-over-states density-functional perturbation theory (SOS-DFPT) calculations, as implemented in the *deMON-NMR* program (Malkin *et al.* (1996) and references therein). Two sets of structures were used for the calculations: one set consisted of the starting structure shown in figure 4*a*, where the valine side-chain χ_1 angle was incremented in steps of 5°, while keeping the rest of the fragment unchanged; the second set consisted of the same starting structure, but the structures resulting from each χ_1 increment were energy minimized using the computer program CHARMM24 (Brooks *et al.* 1983) with dihedral angle constraints for χ_1. Calculations were also performed on a larger fragment, which included all atoms within a 5 Å radius of the valine residue to ensure that the surroundings were correctly taken into account. No changes in the chemical shifts were found between this latter fragment and the one shown in figure 4*a*, indicating that the atoms considered in figure 4*a* form a complete minimal set. The resulting calculated chemical shifts are shown in figure 4*b*,*c*, by the open circles for each χ_1 increment. The circles in green correspond to the valine $C^{\gamma 1}$ shifts, whereas the ones in red correspond to the $C^{\gamma 2}$ shifts. The black crosses correspond to the experimental shifts found for the two valine side-chain rotamers in antamanide (Straus *et al.* 1997). The best fit between calculated and experimental shifts yields an estimate for the dihedral angles: $\chi_1 = -50°$ for rotamer I and $\chi_1 = 203°$ for rotamer II (rotamer III is not observed). This is in agreement with other findings reported in Straus *et al.* (1997) and could be reinforced by using methods to determine torsion angles, as outlined in the following subsection.

(b) *Torsion angles*

Recently a number of solid-state NMR experiments (Costa *et al.* 1997; Hong *et al.* 1997, 1998; Feng *et al.* 1997; Reif *et al.* 2000; Takegoshi *et al.* 2000; Baldus 2002; Ladizhansky *et al.* 2002; Rienstra *et al.* 2002*b*) have been proposed, which allow the direct measurement of torsion angles (ϕ, ψ, χ_1). By measuring these dihedral angles, the peptide backbone and side-chain conformation can be determined (figure 5), and thus the secondary structure. All the methods given above rely on the angular

dependence of the dipolar and chemical shift tensors and result in a measurement of the relative orientation between two tensors (e.g. dipolar vector relative to another dipolar vector). To get the full geometry of the peptide from this relative angle measurement, assumptions on bond angle and bond lengths need to be made. When applying these techniques to fully labelled peptides and proteins, the spectral resolution and the sensitivity must be sufficiently high. Rienstra *et al.* (2002*b*) demonstrated how some of these sequences can be applied to the uniformly $^{13}C/^{15}N$-labelled tripeptide formyl–Met–Leu–Phe–OH. A number of torsion angles (3ϕ, 2ψ, $3\chi_1$ angles shown in figure 5) were determined from a combination of 3D experiments, each relating different dipolar vectors to one another. For example, to determine ϕ, the relative $^{1}H–^{13}C$ and $^{1}H–^{15}N$ dipolar vector orientations were measured using a 3D $^{1}H–^{15}N–^{13}CA–^{1}HA$ experiment. The conformation is obtained by comparing simulated spectra with experimental ones.

To date, there are no examples in the literature of the direct application of these methods to larger peptides (more than three amino acid residues) and proteins. The approach used for these larger systems, touched upon in the previous section, is to compare experimentally determined chemical shifts with databases that correlate chemical shifts with backbone torsion angles. Two examples of this methodology, both applied to amyloid fibrils, are given in Jaroniec *et al.* (2002) and Petkova *et al.* (2002). Petkova *et al*. primarily used the TALOS database (Cornilescu *et al.* 1999) to predict ϕ and ψ from ^{13}C and ^{15}N chemical shifts, with some torsion angles being derived from doubly labelled samples. Jaroniec *et al*. complemented their TALOS-based predictions with distance measurements between four $^{13}C–^{15}N$ pairs in two selectively labelled samples. As methods are developed to improve resolution and sensitivity in protein samples, the determination of torsion angles, either from direct methods or from chemical shift data, will be carried out on these biomolecules.

(c) *Distances*

As mentioned in the previous section, distances between pairs of nuclei can yield information on the secondary structure of biological molecules. Many examples exist in the literature where distances between two selectively labelled nuclei are measured. A recent review by Thompson (2002) illustrates a number of examples on the application of distance measurement methods such as rotational-echo double-resonance (REDOR) (Schaefer 1999) and rotational resonance (Levitt *et al.* 1990) to selectively labelled proteins.

For fully labelled peptides and proteins, however, there are comparatively few examples of distance measurements. This is due to the fact that the strong couplings between directly bonded spins (e.g. $^{13}C–^{13}C$ scalar couplings) in fully labelled systems interfere with the weak couplings needed to get distance information in the range 3–6 Å. One approach to eliminate the homonuclear scalar couplings in fully labelled systems is to apply a frequency-selective spin-echo (Straus *et al.* 1996). Jaroniec *et al.* (1999) incorporated this pulse sequence element into a REDOR experiment, resulting in the accurate measurement of the distance between C^{γ} and N in uniformly labelled threonine. Subsequent work by the same group yielded an improved experiment that suppresses all $^{13}C–^{15}N$ and $^{13}C–^{13}C$ interactions, other than the individual $^{13}C–^{15}N$ dipolar couplings (Jaroniec *et al.* 2001*a*). When applied to the fully $^{13}C/^{15}N$-labelled tripeptide *N*-formyl–Met–Leu–Phe–OH, this approach yielded a total of 16 $^{13}C–^{15}N$ distances that could be measured from a single sample. Recall that if pairs of labels were to be used instead, this would require the synthesis and purification of a large number of samples (up to 16). Secondary structure information can also be obtained from the semi-quantitative measurement of $^{13}C–^{13}C$ and $^{15}N–^{15}N$ distances, as recently described in Castellani *et al.* (2002). Distance restraints are obtained from proton-driven spin diffusion correlation experiments, recorded at different mixing times, in a manner analogous to nuclear Overhauser effect (NOE) buildups in solution-state NMR. The peak intensities are compared with reference values, classified in different ranges and used as restraints in the structure calculation. This approach resulted in the first structure determination of a protein by solid-state NMR, without recourse to any information from other methods.

Distance measurements could potentially also yield tertiary structure information on peptides and proteins. Recently, several examples in the literature demonstrated how solid-state MAS NMR can be used to probe hydrogen bond distances. Some of the approaches rely on either $^{13}C–^{1}H$ (Van Rossum *et al.* 2000) or $^{15}N–^{1}H$ (Zhao *et al.* 2001) distance measurements in model systems. Other recent work by Lange *et al.* (2002) and Tycko & Ishii (2003) elegantly demonstrate how $^{1}H–^{1}H$ distances can be measured in fully $^{13}C/^{15}N$-labelled ubiquitin and amyloid fibrils, respectively.

5. CONCLUSIONS AND OUTLOOK

The recent developments in the field of solid-state MAS NMR outlined in this review clearly indicate how this technique can be applied to fully isotopically labelled peptides and proteins. To undertake a successful study, sufficient resolution must first be attained. This can be done by choosing the appropriate labelling scheme and by recrystallization or precipitation of the sample to yield micro- or nanocrystals. Once the sample is prepared, a number of assignment strategies can be used to identify the individual resonances. Parameters, such as labelling, sensitivity and resolution, must all be taken into account when choosing the appropriate assignment method. Finally, once the spectra are assigned, secondary structure can be determined by using either chemical shift information, torsion angle measurements or distance measurements. Current and future combined use of high-field spectrometers (greater than or equal to 600 MHz), MAS probes capable of fast spinning speeds (Samoson *et al.* 2001) and of handling high power (Martin *et al.* 2003), and methods to preserve the integrity of the biological samples (Martin *et al.* 2003), will all lead to a number of structures, solved using solid-state NMR, being reported. Indeed, recent applications of the MAS methods reported here to fully $^{13}C/^{15}N$-labelled membrane proteins (Jaroniec *et al.* 2001*b*) and amyloid fibrils (Jaroniec *et al.* 2002; Petkova *et al.* 2002) clearly indicate that solid-state NMR will play an important part in the characterization of protein structure in the future.

Solid-state NMR is thus expected to become increasingly important to tackle a wide range of biophysical problems: from the characterization of the conformation of small peptides and ligands bound to larger proteins (e.g. receptors) to the full characterization of the 3D structure of biopolymers in noncrystalline solid forms, such as membrane proteins, amyloid proteins and cellulose.

The author gratefully acknowledges Walter R. P. Scott and Hélène Martel for carefully reading through this manuscript and for helpful discussions. The author also thanks The Royal Society for their past support in the form of a Dorothy Hodgkin Research Fellowship and the Natural Sciences and Engineering Research Council of Canada for a University Faculty Award.

ENDNOTES

[1]The term 'selective' is used in this instance as in the literature. In this case, 'selective' refers to one or more labels in each amino acid in the peptide or protein, as opposed to a few labels scattered throughout the sample.

[2]Other spectroscopic parameters were different in the two studies.

REFERENCES

Alla, M. & Lippmaa, E. 1982 Resolution limits in magic-angle rotation NMR spectra of polycrystalline samples. *Chem. Phys. Lett.* **87**, 30–33.

Anand, K., Pal, D. & Hilgenfeld, R. 2002 An overview on 2-methyl-2,4-pentanediol in crystallization and in crystals of biological macromolecules. *Acta Crystallogr. D Biol. Crystallogr.* **58**, 1722–1728.

Arakawa, T., Bhat, R. & Timasheff, S. N. 1990 Why preferential hydration does not always stabilize the native structure of globular proteins. *Biochemistry* **29**, 1924–1931.

Astrof, N. S. & Griffin, R. G. 2002 Soft triple resonance solid-state NMR experiments for assignments of U-^{13}C, ^{15}N labeled peptides and proteins. *J. Magn. Reson.* **158**, 157–163.

Astrof, N. S., Lyon, C. E. & Griffin, R. G. 2001 Triple resonance solid state NMR experiments with reduced dimensionality evolution periods. *J. Magn. Reson.* **152**, 303–307.

Baldus, M. 2002 Correlation experiments for assignment and structure elucidation of immobilized polypeptides under magic angle spinning. *Prog. Nucl. Magn. Reson.* **41**, 1–47.

Baldus, M. & Meier, B. H. 1996 Total correlation spectroscopy in the solid state. The use of scalar couplings to determine the through-bond connectivity. *J. Magn. Reson.* A **121**, 65–69.

Baldus, M., Geurts, D. G., Hediger, S. & Meier, B. H. 1996 Efficient N-15–C-13 polarization transfer by adiabatic-passage Hartmann–Hahn cross polarization. *J. Magn. Reson.* A **118**, 140–144.

Baldus, M., Petkova, A. T., Herzfeld, J. & Griffin, R. G. 1998 Cross polarization in the tilted frame: assignment and spectral simplification in heteronuclear spin systems. *Mol. Phys.* **95**, 1197–1207.

Belton, P. S., Gil, A. M. & Tanner, S. F. 1993 Factors affecting the line widths and signal-to-noise ratios of the C-13 CP/MAS spectra of proteins. *Magn. Reson. Chem.* **31**, 1001–1007.

Bennett, A. E., Ok, J. H., Griffin, R. G. & Vega, S. 1992 Chemical-shift correlation spectroscopy in rotating solids: radio frequency driven dipolar recoupling and longitudinal exchange. *J. Chem. Phys.* **96**, 8624–8627.

Berry, M. B. 1995 Structure and dynamics of *E. coli* adenylate kinase. PhD thesis, Rice University, Houston, TX, chapters 2–3.

Blaschke, U. K., Cotton, G. J. & Muir, T. W. 2000 Synthesis of multi-domain proteins using expressed protein ligation: strategies for segmental isotopic labeling of internal regions. *Tetrahedron* **56**, 9461–9470.

Brender, J. R., Taylor, D. M. & Ramamoorthy, A. 2001 Orientation of amide-nitrogen-15 chemical shift tensors in peptides: a quantum chemical study. *J. Am. Chem. Soc.* **123**, 914–922.

Brooks, B. R., Bruccoleri, R. E., Olafson, B. D., States, D. J., Swaminathan, S. & Karplus, M. 1983 CHARMM: a program for macromolecular energy, minimization, and dynamics calculations. *J. Comp. Chem.* **4**, 187–217.

Brutscher, B., Simorre, J. P., Caffrey, M. S. & Marion, D. 1994 Design of a complete set of two-dimensional triple-resonance experiments for assigning labeled proteins. *J. Magn. Reson.* B **105**, 77–82.

Brutscher, B., Cordier, F., Simorre, J. P., Caffrey, M. S. & Marion, D. 1995 High resolution 3D HNCOCA experiment applied to a 28 kDa paramagnetic protein. *J. Biomol. NMR* **5**, 202–206.

Burley, S. K. 2000 An overview of structural genomics. *Nature Struct. Biol.* **7**, 932–934.

Case, D. A. 2000 Interpretation of chemical shifts and coupling constants in macromolecules. *Curr. Opin. Struct. Biol.* **10**, 197–203.

Castellani, F., Van Rossum, B. J., Diehl, A., Schubert, M., Rehbein, K. & Oschkinat, H. 2002 Structure of a protein determined by solid-state magic-angle NMR spectroscopy. *Nature* **420**, 98–102.

Cegelski, L., Kim, S. J., Hing, A. W., Studelska, D. R., O'Connor, R. D., Mehta, A. K. & Schaefer, J. 2002 Rotational-echo double resonance characterization of the effects of vancomycin on cell wall synthesis in *Staphylococcus aureus*. *Biochemistry* **41**, 13 053–13 058.

Cornilescu, G., Delaglio, F. & Bax, A. 1999 Protein backbone angle restraints from searching a database for chemical shift and sequence homology. *J. Biomol. NMR* **13**, 289–302.

Costa, P. R., Gross, J. D., Hong, M. & Griffin, R. G. 1997 Solid-state NMR measurement of Psi in peptides: a NCCN 2Q-heteronuclear local field experiment. *Chem. Phys. Lett.* **280**, 95–103.

Cowburn, D. & Muir, T. W. 2001 Segmental isotopic labeling using expressed protein ligation. *Meth. Enzymol.* **339**, 41–54.

Croasmun, W. R. & Carlson, R. M. K. (eds) 1994 *Two-dimensional NMR spectroscopy*, 2nd edn. New York: VCH Publishers, Inc.

Davis, J. H. & Auger, M. 1999 Static and magic angle spinning NMR of membrane peptides and proteins. *Prog. Nucl. Magn. Reson.* **35**, 1–84.

de Groot, H. J. M. 2000 Solid state NMR spectroscopy applied to membrane proteins. *Curr. Opin. Struct. Biol.* **10**, 593–600.

Detken, A., Hardy, E. H., Ernst, M., Kainosho, M., Kawakami, T., Aimoto, S. & Meier, B. H. 2001 Methods for sequential resonance assignment in solid, uniformly C-13, N-15 labelled peptides: quantification and application to antamanide. *J. Biomol. NMR* **20**, 203–221.

Feng, X., Edén, M., Brinkmann, A., Luthman, H., Eriksson, L., Gräslund, A., Antzutkin, O. N. & Levitt, M. H. 1997 Direct determination of a peptide torsional angle by solid-state NMR. *J. Am. Chem. Soc.* **119**, 12 006–12 007.

Gardner, K. H. & Kay, L. E. 1998 The use of H-2, C-13, N-15 multidimensional NMR to study the structure and dynamics of proteins. *A. Rev. Biophys. Biomol. Struct.* **27**, 357–406.

Geahigan, K. B., Meints, G. A., Hatcher, M. E., Orban, J. & Drobny, G. P. 2000 The dynamic impact of CpG methylation in DNA. *Biochemistry* **39**, 4939–4946.

Goto, N. K. & Kay, L. E. 2000 New developments in isotope labeling strategies for protein solution NMR spectroscopy. *Curr. Opin. Struct. Biol.* **10**, 585–592.

Goto, N. K., Gardner, K. H., Mueller, G. A., Willis, R. C. & Kay, L. E. 1999 A robust and cost-effective method for the production of Val, Leu, Ile$^{\delta 1}$ methyl-protonated N-15-, C-13-, H-2-labeled proteins. *J. Biomol. NMR* **13**, 369–374.

Gregory, D. M., Mitchell, D. J., Stringer, J. A., Kiihne, S., Shiels, J. C., Callahan, J., Mehta, M. A. & Drobny, G. P. 1995 Windowless dipolar recoupling: the detection of weak dipolar couplings between spin-1/2 nuclei with large chemical-shift anisotropies. *Chem. Phys. Lett.* **246**, 654–663.

Griffin, R. G. 1998 Dipolar recoupling in MAS spectra of biological solids. *Nature Struct. Biol.* **5**, 508–512.

Gu, Z. T. & Opella, S. J. 1999 Two- and three-dimensional ^{1}H/^{13}C PISEMA experiments and their application to backbone and side chain sites of amino acids and peptides. *J. Magn. Reson.* **140**, 340–346.

Havlin, R. H., Le, H., Laws, D. D., deDios, A. C. & Oldfield, E. 1997 An *ab initio* quantum chemical investigation of carbon-13 NMR shielding tensors in glycine, alanine, valine, isoleucine, serine and threonine: comparisons between helical and sheet tensors, and the effects of χ_1 on shielding. *J. Am. Chem. Soc.* **119**, 11 951–11 958.

Hong, M. 1999*a* Determination of multiple phi-torsion angles in proteins by selective and extensive ^{13}C labeling and two-dimensional solid state NMR. *J. Magn. Reson.* **139**, 389–401.

Hong, M. 1999*b* Resonance assignment of C-13/N-15 labeled solid proteins by two- and three-dimensional magic-angle-spinning NMR. *J. Biomol. NMR* **15**, 1–14.

Hong, M. 2000 Solid-state NMR determination of ^{13}Cα chemical shift anisotropies for the identification of protein secondary structure. *J. Am. Chem. Soc.* **122**, 3762–3770.

Hong, M. & Jakes, J. 1999 Selective and extensive ^{13}C labeling of a membrane protein for solid state NMR investigations. *J. Biomol. NMR* **14**, 71–74.

Hong, M., Gross, J. D. & Griffin, R. G. 1997 Site-resolved determination of peptide torsion angle phi from the relative orientations of backbone N-H and C-H bonds by solid-state NMR. *J. Phys. Chem.* B **101**, 5869–5874.

Hong, M., Gross, J. D., Hu, W. & Griffin, R. G. 1998 Determination of the peptide torsion angle phi by N-15 chemical shift and C-13α-H-1α dipolar tensor correlation in solid-state MAS NMR. *J. Magn. Reson.* **135**, 169–177.

Ishii, Y., Yesinowski, J. P. & Tycko, R. 2001 Sensitivity enhancement in solid-state ^{13}C NMR of synthetic polymers and biopolymers by ^{1}H NMR detection with high-speed magic angle spinning. *J. Am. Chem. Soc.* **123**, 2921–2922.

Jakeman, D. L., Mitchell, D. J., Shuttleworth, W. A. & Evans, J. N. S. 1998 Effects of sample preparation conditions on biomolecular solid-state NMR lineshapes. *J. Biomol. NMR* **12**, 417–421.

Jaroniec, C. P., Tounge, B. A., Rienstra, C. M., Herzfeld, J. & Griffin, R. G. 1999 Measurement of C-13–N-15 distances in uniformly C-13 labeled biomolecules: J-decoupled REDOR. *J. Am. Chem. Soc.* **121**, 10 237–10 238.

Jaroniec, C. P., Tounge, B. A., Herzfeld, J. & Griffin, R. G. 2001*a* Frequency selective heteronuclear dipolar recoupling in rotating solids: accurate C-13–N-15 distance measurements in uniformly C-13,N-15-labeled peptides. *J. Am. Chem. Soc.* **123**, 3507–3519.

Jaroniec, C. P., Lansing, J. C., Tounge, B. A., Belenky, M., Herzfeld, J. & Griffin, R. G. 2001*b* Measurement of dipolar couplings in a uniformly ^{13}C, ^{15}N-labeled membrane protein: distances between the Schiff base and aspartic acids in the active site of bacteriorhodopsin. *J. Am. Chem. Soc.* **123**, 12 929–12 930.

Jaroniec, C. P., MacPhee, C. E., Astrof, N. S., Dobson, C. M. & Griffin, R. G. 2002 Molecular conformation of a peptide fragment of transthyretin in an amyloid fibril. *Proc. Natl Acad. Sci. USA* **99**, 16 748–16 753.

Karle, I. 1986 Water structure in [Phe^{4} Val^{6}] antamanide.12 H_2O crystallized from dioxane. *Int. J. Pept. Protein Res.* **28**, 6–14.

Ketchem, R. R., Lee, K. C., Huo, S. & Cross, T. A. 1996 Macromolecular structural elucidation with solid-state NMR-derived orientational constraints. *J. Biomol. NMR* **8**, 1–14.

Labudde, D., Leitner, D., Kruger, M. & Oschkinat, H. 2003 Prediction algorithm for amino acid types with their secondary structure in proteins (PLATON) using chemical shifts. *J. Biomol. NMR* **25**, 41–53.

Ladizhansky, V., Veshtort, M. & Griffin, R. G. 2002 NMR determination of the torsion angle Psi in alpha-helical peptides and proteins: the HCCN dipolar correlation experiment. *J. Magn. Reson.* **154**, 317–324.

Lange, A., Luca, S. & Baldus, M. 2002 Structural constraints from proton-mediated rare-spin correlation spectroscopy in rotating solids. *J. Am. Chem. Soc.* **124**, 9704–9705.

Lee, H., Ortiz de Montellano, P. R. & McDermott, A. E. 1999 Deuterium magic angle spinning studies of substrates bound to cytochrome P450. *Biochemistry* **38**, 10 808–10 813.

Lee, K. M., Androphy, E. J. & Baleja, J. D. 1995 A novel method for selective isotope labeling of bacterially expressed proteins. *J. Biomol. NMR* **5**, 93–96.

Lee, Y. K., Kurur, N. D., Helmle, M., Johannessen, O. G., Nielsen, N. C. & Levitt, M. H. 1995 Efficient dipolar recoupling in the NMR of rotating solids: a sevenfold symmetrical radio frequency pulse sequence. *Chem. Phys. Lett.* **242**, 304–309.

LeMaster, D. M. 1994 Isotope labeling in solution protein assignment and structural analysis. *Prog. Nucl. Magn. Reson.* **26**, 371–419.

Lesage, A., Auger, C., Caldarelli, S. & Emsley, L. 1997 Determination of through-bond carbon–carbon connectivities in solid-state NMR using the INADEQUATE experiment. *J. Am. Chem. Soc.* **119**, 7867–7868.

Levitt, M. H., Raleigh, D., Creuzet, F. & Griffin, R. G. 1990 Theory and simulations of homonuclear spin pair systems in rotating solids. *J. Chem. Phys.* **92**, 6347–6364.

Luca, S. & Baldus, M. 2002 Enhanced spectral resolution in immobilized peptides and proteins by combining chemical shift sum and difference spectroscopy. *J. Magn. Reson.* **159**, 243–249.

Ma, C., Marassi, F. M., Jones, D. H., Straus, S. K., Bour, S., Schubert, U., Strebel, K., Oblatt-Montal, M., Montal, M. & Opella, S. J. 2002 Expression, purification, and activities of full-length and truncated versions of the integral membrane protein Vpu from HIV-1. *Protein Sci.* **11**, 546–557.

McDermott, A. 2002 Studies of TIM and other enzymes by solid state NMR. Presented at the recent innovations in biological solid state NMR meeting, September 2–3, Oxford.

McDermott, A., Polenova, T., Bockmann, A., Zilm, K. W., Paulsen, E. K., Martin, R. W. & Montelione, G. T. 2000 Partial NMR assignments of uniformly (C-13,N-15)-enriched BPTI in the solid state. *J. Biomol. NMR* **16**, 209–219.

Malkin, V. G., Malkina, O. L. & Salahub, D. R. 1996 Spin-orbit correction to NMR shielding constants from density functional theory. *Chem. Phys. Lett.* **261**, 335–345.

Marassi, F. M. & Opella, S. J. 2003 Simultaneous assignment and structure determination of a membrane protein from NMR orientational restraints. *Protein Sci.* **12**, 403–411.

Martin, R. W., Paulsen, E. K. & Zilm, K. W. 2003 Design of a triple resonance magic angle sample spinning probe for high field solid state nuclear magnetic resonance. *Rev. Sci. Instrum.* **74**, 3045–3061.

Maunu, S. L. 2002 NMR studies of wood and wood products. *Prog. Nucl. Magn. Reson.* **40**, 151–174.

Middleton, D. A., Rankin, S., Esmann, M. & Watts, A. 2000 Structural insights into the binding of cardiac glycosides to the digitalis receptor revealed by solid-state NMR. *Proc. Natl Acad. Sci. USA* **97**, 13 602–13 607.

Moltke, S., Wallat, I., Sakai, N., Nakanishi, K., Brown, M. F. & Heyn, M. P. 1999 The angles between the C-1-, C-5- and C-9-methyl bonds of the retinylidene chromophore and the membrane normal increase in the M intermediate of bacteriorhodopsin: direct determination with solid-state H-2 NMR. *Biochemistry* **38**, 11 762–11 772.

Morgan, W. D., Kragt, A. & Feeney, J. 2000 Expression of deuterium-isotope-labelled protein in the yeast *Pichia pastoris* for NMR studies. *J. Biomol. NMR* **17**, 337–347.

Nielsen, N. C., Bildsoe, H., Jakobsen, H. J. & Levitt, M. H. 1994 Double-quantum homonuclear rotary resonance: efficient dipolar recovery in magic-angle-spinning nuclear magnetic resonance. *J. Chem. Phys.* **101**, 1805–1812.

Nishimura, K., Kim, S., Zhang, L. & Cross, T. A. 2002 The closed state of a H^+ channel helical bundle combining precise orientational and distance restraints from solid state NMR. *Biochemistry* **41**, 13 170–13 177.

Nomura, K., Takegoshi, K., Terao, T., Uchida, K. & Kainosho, M. 2000 Three-dimensional structure determination of a uniformly labeled molecule by frequency-selective dipolar recoupling under magic-angle spinning. *J. Biomol. NMR* **17**, 111–123.

Opella, S. J. 1997 NMR and membrane proteins. *Nature Struct. Biol.* **4S**, 845–848.

Opella, S. J., Marassi, F. M., Gesell, J. J., Valente, A. P., Kim, Y., Oblatt-Montal, M. & Montal, M. 1999 Structures of the M2 channel-lining segments from nicotinic acetylcholine and NMDA receptors by NMR spectroscopy. *Nature Struct. Biol.* **6**, 374–379.

Otomo, T., Teruya, K., Uekagi, K., Yamazaki, T. & Kyogoku, Y. 1999*a* Improved segmental isotope labeling of proteins and application to a larger protein. *J. Biomol. NMR* **14**, 105–114.

Otomo, T., Ito, N., Kyogoku, Y. & Yamazaki, T. 1999*b* NMR observation of selected segments in a larger protein: central-segment isotope labeling through intein-mediated ligation. *Biochemistry* **38**, 16 040–16 044.

Ottleben, H., Haasemann, M., Ramachandran, R., Muller-Esterl, W. & Brown, L. R. 1997 NMR investigations of recombinant N-15/C-13/H-2-labeled bradykinin bound to a Fab mimic of the B2 receptor. *Receptors Channels* **5**, 237–241.

Pauli, J., Van Rossum, B., Forster, H., de Groot, H. J. M. & Oschkinat, H. 2000 Sample optimization and identification of signal patterns of amino acid side chains in 2D RFDR spectra of the alpha-spectrin SH3 domain. *J. Magn. Reson.* **143**, 411–416.

Pauli, J., Baldus, M., Van Rossum, B., de Groot, H. J. M. & Oschkinat, H. 2001 Backbone and side-chain ^{13}C and ^{15}N signal assignments of the α-spectrin SH3 domain by magic angle spinning solid-state NMR at 17.6 Tesla. *Chem. Biol. Chem.* **2**, 272–281.

Perler, F. B. 1998 Protein splicing of inteins and hedgehog autoproteolysis: structure, function, and evolution. *Cell* **92**, 1–4.

Petkova, A. T., Ishii, Y., Balbach, J. J., Antzutkin, O. N., Leapman, R. D., Delaglio, F. & Tycko, R. 2002 A structural model for Alzheimer's beta-amyloid fibrils based on experimental constraints from solid state NMR. *Proc. Natl Acad. Sci. USA* **99**, 16 742–16 747.

Ramamoorthy, A., Fujiwara, T. & Nagayama, K. 1993 An rf pulse sequence optimized for homonuclear-J cross-polarization under magic-angle spinning conditions in solids. *J. Magn. Reson.* **A104**, 366–368.

Reif, B., Hohwy, M., Jaroniec, C. P., Rienstra, C. M. & Griffin, R. G. 2000 NH-NH vector correlation in peptides by solid-state NMR. *J. Magn. Reson.* **145**, 132–141.

Reif, B., Jaroniec, C. P., Rienstra, C. M., Hohwy, M. & Griffin, R. G. 2001 ^1H-^1H MAS correlation spectroscopy and distance measurements in a deuterated peptide. *J. Magn. Reson.* **151**, 320–327.

Richter, G., Kelly, M., Krieger, C., Yu, Y., Bermel, W., Karlsson, G., Bacher, A. & Oschkinat, H. 1999 NMR studies on the 46 kDa dimeric protein, 3,4-dihydroxy-2-butanone 4-phosphate synthase, using H-2, C-13, and N-15-labelling. *Eur. J. Biochem.* **261**, 57–65.

Rienstra, C. M., Tucker-Kellogg, L., Jaroniec, C. P., Hohwy, M., Reif, B., McMahon, M. T., Tidor, B., Lozano-Perez, T. & Griffin, R. G. 2002*a* *De novo* determination of peptide structure with solid-state magic-angle spinning NMR spectroscopy. *Proc. Natl Acad. Sci. USA* **99**, 10 260–10 265.

Rienstra, C. M., Hohwy, M., Mueller, L. J., Jaroniec, C. P., Reif, B. & Griffin, R. G. 2002*b* Determination of multiple torsion-angle constraints in U-C-13,N-15-labeled peptides: 3D H-1–N-15–C-13–H-1 dipolar chemical shift NMR spectroscopy in rotating solids. *J. Am. Chem. Soc.* **124**, 11 908–11 922.

Saito, H., Tuzi, S., Yamaguchi, S., Tanio, M. & Naito, A. 2000 Conformation and backbone dynamics of bacteriorhodopsin revealed by C13 NMR. *BBA Bioenergetics* **1460**, 39–48.

Samoson, A., Tuherm, T. & Gan, Z. 2001 High-field high-speed MAS resolution enhancement in ^1H NMR spectroscopy of solids. *Solid State Nucl. Magn. Reson.* **20**, 130–136.

Schaefer, J. 1999 REDOR-determined distances from hetero-spins to clusters of C-13 labels. *J. Magn. Reson.* **137**, 272–275.

Schnell, I. & Spiess, H. W. 2001 High-resolution H-1 NMR spectroscopy in the solid state: very fast sample rotation and multiple-quantum coherences. *J. Magn. Reson.* **151**, 153–227.

Schwerk, U., Michel, D. & Pruski, M. 1996 Local magnetic field distribution in a polycrystalline sample exposed to a strong magnetic field. *J. Magn. Reson.* **A119**, 157–164.

Shan, X., Gardner, K. H., Muhandiram, D. R., Kay, L. E. & Arrowsmith, C. H. 1998 Subunit-specific backbone NMR assignments of a 64 kDa trp repressor DNA complex: a role for N-terminal residues in tandem binding. *J. Biomol. NMR* **11**, 307–318.

Shoji, A., Ando, S., Kuroki, S., Ando, I. & Webb, G. A. 1993 Structural studies of peptides and polypeptides in the solid state by ^{15}N NMR. *A. Rep. NMR Spect.* **26**, 55–98.

Smith, S. O., Aschheim, K. A. & Groesbeek, M. 1996 Magic angle spinning NMR spectroscopy of membrane proteins. *Q. Rev. Biophys.* **29**, 395–449.

Straus, S. K. 1998 Development and application of techniques for improving resolution in solid state NMR of fully labeled biomolecules. PhD thesis, Eidgenössische Technische Hochschule Zürich, Dissertation No. 12587.

Straus, S. K., Bremi, T. & Ernst, R. R. 1996 Resolution enhancement by homonuclear J decoupling in solid-state MAS NMR. *Chem. Phys. Lett.* **262**, 709–715.

Straus, S. K., Bremi, T. & Ernst, R. R. 1997 Side-chain conformation and dynamics in a solid peptide: CP-MAS NMR study of valine rotamers and methyl-group relaxation in fully C-13-labelled antamanide. *J. Biomol. NMR* **10**, 119–128.

Straus, S. K., Bremi, T. & Ernst, R. R. 1998 Experiments and strategies for the assignment of fully C-13/N-15-labelled polypeptides by solid state NMR. *J. Biomol. NMR* **12**, 39–50.

Stryer, L. 1988 *Biochemistry*, 3rd edn. New York: W. H. Freeman and Company.

Studelska, D. R., Klug, C. A., Beusen, D. D., McDowell, L. M. & Schaefer, J. 1996 Long-range distance measurements of protein binding sites by rotational-echo double-resonance NMR. *J. Am. Chem. Soc.* **118**, 5476–5477.

Sun, B. Q., Costa, P. R., Kocisko, D., Lansbury, P. T. & Griffin, R. G. 1995*a* Internuclear distance measurements in solid-state nuclear magnetic resonance: dipolar recoupling via rotor synchronized spin locking. *J. Chem. Phys.* **102**, 702–707.

Sun, B. Q., Costa, P. R. & Griffin, R. G. 1995 Heteronuclear polarization transfer by radiofrequency-driven dipolar recoupling under magic-angle spinning. *J. Magn. Reson.* A **112**, 191–198.

Suter, D. & Ernst, R. R. 1985 Spin diffusion in resolved solid-state NMR spectra. *Phys. Rev.* B **32**, 5608–5627.

Szyperski, T., Wider, G., Bushweller, J. H. & Wüthrich, K. 1993 Reduced dimensionality in triple-resonance NMR experiments. *J. Am. Chem. Soc.* **115**, 9307–9308.

Takegoshi, K., Imaizumi, T. & Terao, T. 2000 One- and two-dimensional C-13–H-1/N-15–H-1 dipolar correlation experiments under fast magic-angle spinning for determining the peptide dihedral angle phi. *Solid State NMR* **16**, 271–278.

Thompson, L. K. 2002 Solid-state NMR studies of the structure and mechanisms of proteins. *Curr. Opin. Struct. Biol.* **12**, 661–669.

Tycko, R. 2001 Biomolecular solid state NMR: advances in structural methodology and applications to peptide and protein fibrils. *A. Rev. Phys. Chem.* **52**, 575–606.

Tycko, R. & Ishii, Y. 2003 Constraints on supramolecular structure in amyloid fibrils from two-dimensional solid-state NMR spectroscopy with uniform isotopic labelling. *J. Am. Chem. Soc.* **125**, 6606–6607.

Tycko, R. & Smith, S. O. 1993 Symmetry principles in the design of pulse sequences for structural measurements in magic angle spinning nuclear magnetic resonance. *J. Chem. Phys.* **98**, 932–943.

Van Beek, J. D., Hess, S., Vollrath, F. & Meier, B. H. 2002 The molecular structure of spider dragline silk: folding and orientation of the protein backbone. *Proc. Natl Acad. Sci. USA* **99**, 10 266–10 271.

Van Rossum, B. J., Förster, H. & de Groot, H. J. M. 1997 High-field and high-speed CPMAS ^{13}C NMR heteronuclear dipolar-correlation spectroscopy of solids with frequency-switched Lee–Goldburg homonuclear decoupling. *J. Magn. Reson.* **124**, 516–519.

Van Rossum, B. J., de Groot, C. P., Ladizhansky, V., Vega, S. & de Groot, H. J. M. 2000 A method for measuring heteronuclear (H-1–C-13) distances in high speed MAS NMR. *J. Am. Chem. Soc.* **122**, 3465–3472.

Van Rossum, B. J., Schulten, E. A. M., Raap, J., Oschkinat, H. & de Groot, H. J. M. 2002 A 3-D structural model of solid self-assembled chlorophyll *a*/H_2O from multispin labeling and MAS NMR 2-D dipolar correlation spectroscopy in high magnetic field. *J. Magn. Reson.* **155**, 1–14.

Verel, R., Baldus, M., Ernst, M. & Meier, B. H. 1998 A homonuclear spin-pair filter for solid-state NMR based on adiabatic-passage techniques. *Chem. Phys. Lett.* **287**, 421–428.

Vinogradov, E., Madhu, P. K. & Vega, S. 2002 Proton spectroscopy in solid state nuclear magnetic resonance with windowed phase modulated Lee–Goldburg decoupling sequences. *Chem. Phys. Lett.* **354**, 193–202.

Wang, J., Kim, S., Kovacs, F. & Cross, T. A. 2001 Structure of the transmembrane region of the M2 protein H^+ channel. *Protein Sci.* **10**, 2241–2250.

Watts, J. A., Watts, A. & Middleton, D. A. 2001 A model of reversible inhibitors in the gastric H^+/K^+-ATPase binding site determined by rotational echo double resonance NMR. *J. Biol. Chem.* **276**, 43 197–43 204.

Wei, Y., de Dios, A. C. & McDermott, A. E. 1999 Solid-state ^{15}N NMR chemical shift anisotropy of histidines: experimental and theoretical studies of hydrogen bonding. *J. Am. Chem. Soc.* **121**, 10 389–10 394.

Wieland, T. & Bodanszky, M. 1991 *The world of peptides: a brief history of peptide chemistry*. Berlin: Springer.

Williamson, P. T. F., Bains, S., Chung, C., Cooke, R. & Watts, A. 2002 Probing the environment of neurotensin whilst bound to the neurotensin receptor by solid state NMR. *FEBS Lett.* **518**, 111–115.

Wishart, D. S., Sykes, B. D. & Richards, F. M. 1991 Relationship between nuclear magnetic resonance chemical shift and protein secondary structure. *J. Mol. Biol.* **222**, 311–333.

Yamazaki, T., Otomo, T., Oda, N., Kyogoku, Y., Uegaki, K., Ito, N., Ishino, Y. & Nakamura, H. 1998 Segmental isotope labelling for protein NMR using peptide splicing. *J. Am. Chem. Soc.* **120**, 5591–5592.

Zhao, X., Sudmeier, J. L., Bachovchin, W. W. & Levitt, M. H. 2001 Heteronuclear recoupling in fast magic-angle spinning solid-state NMR spectroscopy. Measurement of NH bond lengths and quantification of hydrogen bonds. *J. Am. Chem. Soc.* **123**, 11 097–11 098.